Resilient Quadratic Time-Frequency Distribution for FM Signals with Gapped Missing Data

Yimin D. Zhang

Department of Electrical and Computer Engineering
Temple University, Philadelphia, PA 19122, USA

***Abstract*—Frequency modulated (FM) signals are frequently encountered in radar signal processing. In practice, such signals may experience distortions due to target radar cross section fluctuation, propagation fading, and line-of-sight obstruction. Such distortions make time-frequency presentations and analyses challenging. The problem becomes even more difficult for data with gapped missing samples, i.e., data samples are missing consecutively. In this paper, we address this problem in the context of resilient quadratic time-frequency distributions, which are achieved by applying robust spectrum analysis techniques to the instantaneous autocorrelation functions. In addition, utilization of compressive sensing and sparse reconstruction techniques, in lieu of the conventional Fourier transform, further improves the quality of the estimated time-varying instantaneous frequency signatures.**

***Index Terms*—Radar signal processing, nonstationary signal, time-frequency analysis, missing sample, compressive sensing.**

I. Introduction

Nonstationary frequency modulated (FM) signals with instantaneous narrowband signatures are widely observed in various applications, such as radar, sonar, and radio astronomy [1]. In radar systems, linear frequency modulated (LFM) waveforms are commonly used as sensing signals [2]. The return signals scattering back from moving and maneuvering targets exhibit time-varying Doppler and micro-Doppler signatures, depending on the nature of the target motions [3, 4]. Generally, time-frequency distributions (TFDs) provide effective means for the analysis, characterization, and visualization of such nonstationary signals [5–7].

Time-frequency (TF) analysis methods can be classified into linear transforms and quadratic TFDs (QTFDs). Examples of the former include short-time Fourier transform (STFT), Gabor transform, fractional Fourier transform, and wavelet transform. These transforms represent the nonstationary signal as a weighted sum of atoms or bases that capture the signal local behavior in some ways. QTFDs, also referred to as bilinear TFDs, on the other hand, depict the signal power distribution in the joint TF domain, and generally yield better resolution than their linear transform counterparts. The aim of QTFDs is to concentrate the signal power along the instantaneous frequency (IF) of each signal components. In the case of radar backscattering from a moving target, such concentration accurately reveals the target velocity, acceleration, and higher-order motion behaviours.

In practice, such signals may experience distortions due to, for example, target radar cross section (RCS) fluctuation, propagation fading, line-of-sight obstruction, and interference removal. Such distortions make TF presentations and analyses challenging. Several robust TF analysis methods have been developed based on TF kernels and sparse reconstruction [8–12]. Proper TF kernels, particularly adaptive ones that are optimized with the data, perform two-dimensional (2-D) filtering in the TF domain, thereby effectively reducing the effect of missing samples.

A more challenging situation arises when the missing data occurs consecutively, yielding gapped missing data reception. This may happen when the signal obstruction or fading spans over multi-sample periods. In this case, the above methods generally fail to function well.

In this paper, we address this challenging problem of nonparametric TF analysis of nonstationary FM signals in the context of resilient QTFDs. We notice that, at each time instant, the instantaneous autocorrelation function (IAF) is stationary with respect to the time lag, whereas the Fourier transform of the IAF with respect to the time lag, repeated computed for all time instants, yields the QTFD. As such, resilient QTFDs of nonstationary FM signals can be achieved by applying robust spectrum analysis techniques to recover the missing IAF entries. In particular, we choose the missing data iterative adaptive approach (MIAA) [13] approach as an example to perform missing data recovery in the IAF domain. QTFDs are then obtained by performing Fourier transform of the IAF with respect to the time lag. Alternatively, we can utilize compressive sensing (CS) and sparse reconstruction techniques, in lieu of the Fourier transform, to further improve the quality of the estimated time-varying power spectral signatures. In addition, TF kernels can be applied between the abovementioned two steps to mitigate the effect of cross-terms. All these claims are supported by simulation results.

Notations. A lower (upper) case bold letter denotes a vector (matrix). $(\cdot)^*$ denotes complex conjugation. $\mathcal{F}_x(\cdot)$ and $\mathcal{F}_x^{-1}(\cdot)$ respectively represent the discrete Fourier transform (DFT) and inverse DFT (IDFT) with respect to x. $||\cdot||_1$ denotes the L_1 norm operation. In addition, $\delta(t)$ denotes the Kronecker delta function.

II. Signal Model

A. Signals with Missing Samples

Consider a discrete-time signal, $x(t), t = 1, ..., T$, which comprises a single or multiple components of nonstationary FM signals. Denote $r(t)$ as its observation data with N missing samples, where $0 \leq N < T$. As such, $r(t)$ is the product of $x(t)$ and an "observation mask", $R(t)$, i.e.,

$$r(t) = x(t) \cdot R(t), \tag{1}$$

where

$$R(t) = \begin{cases} 1, & \text{if } t \in \mathbb{S}, \\ 0, & \text{if } t \notin \mathbb{S}. \end{cases} \tag{2}$$

In the above expression, $\mathbb{S} \subset \{1, ..., T\}$ is the set of observed time instants and its cardinality is denoted as $|\mathbb{S}| = T - N$.

For convenience, we denote $X(t) = 1$ for convenience, and define the missing data mask as

$$M(t) = X(t) - R(t) = \sum_{i=1}^{N} \delta(t - t_i), \quad t_i \notin \mathbb{S}. \tag{3}$$

Accordingly, the missing signal is expressed as

$$m(t) = x(t) \cdot M(t) = \sum_{i=1}^{N} x(t)\delta(t - t_i) = \sum_{i=1}^{N} x(t_i)\delta(t - t_i), \tag{4}$$

and the observed data with the missing samples is expressed as

$$r(t) = x(t) - m(t) = x(t) - \sum_{i=1}^{N} x(t_i)\delta(t - t_i). \tag{5}$$

In this paper, as we consider gapped missing data, missing samples are assumed to occur as a single or multiple groups of consecutive missing samples. The number of missing samples in each group is N_0. The positions of the missing sample groups are randomly chosen, and different groups do not overlap. As such, we observe K missing positions, where the total number of missing samples becomes $N = KN_0$.

B. Joint-Variable Domain Representations

The ultimate goal of QTFD analysis is to achieve sharp power concentration in the TF domain on or closely near the true signal IFs. The IAF domain and the ambiguity domain also provide convenient 2-D joint-domain signal representations for signal processing. In particular, TF kernels are designed as multiplicative functions in the ambiguity domain, whereas the stationarity of the IAF facilitates the missing sample recovery as to be discussed in the subsequent section.

The IAF of $x(t)$ is defined as

$$C_{xx}(t, \tau) = x\left(t + \tau\right) x^*\left(t - \tau\right), \tag{6}$$

where τ is the time lag.

The DFT of the IAF $C_{xx}(t, \tau)$ with respect to τ is the well-known Wigner-Ville distribution (WVD), expressed as,

$$W_{xx}(t, f) = \mathcal{F}_\tau[C_{xx}(t, \tau)] = \sum_{\tau} C_{xx}(t, \tau)e^{-j4\pi f \tau}. \tag{7}$$

Note that 4π is used to perform the DFT instead of 2π because the time-lag τ takes integer values. Because $C_{xx}(t, \tau)$ is conjugate symmetric and $C_{RR}(t, \tau)$ is real and symmetric with respect to τ, $C_{rr}(t, \tau)$ is conjugate symmetric with τ as well. As such, the WVD of the observed data, $W_{rr}(t, f) = \mathcal{F}_\tau[C_{rr}(t, \tau)]$, is real-valued.

Applying DFT to the IAF $C_{xx}(t, \tau)$ with respect to t yields the ambiguity function (AF), expressed as,

$$A_{xx}(\theta, \tau) = \mathcal{F}_t[C_{xx}(t, \tau)] = \sum_{t} C_{xx}(t, \tau)e^{-j2\pi\theta t}, \tag{8}$$

where θ is the frequency shift or Doppler. While the AF is mathematically similar to the WVD (performing DFT with respect to t instead of τ), the AF entries are in general complex as the IAF is conjugate symmetric only with τ but not with t. The AF entries are conjugate symmetric with respect to the origin.

III. Effect of Missing Samples and Recovery Techniques

A. Effect of Missing Samples

From (1) and (6), the IAF of $r(t)$ is expressed as

$$C_{rr}(t, \tau) = C_{xx}(t, \tau)C_{RR}(t, \tau), \tag{9}$$

where $C_{RR}(t, \tau)$ is the IAF of the observation mask $R(t)$. To examine the effect of the missing data samples more clearly, we use $R(t) = X(t) - M(t)$ to obtain

$$C_{RR}(t, \tau) = C_{XX}(t, \tau) + C_{MM}(t, \tau) - C_{XM}(t, \tau) - C_{MX}(t, \tau), \tag{10}$$

where $C_{XX}(t, \tau)$ and $C_{MM}(t, \tau)$ are the IAF of $X(t)$ and $M(t)$, respectively, and $C_{XM}(t, \tau)$ and $C_{MX}(t, \tau)$ are two IAF cross-terms between $M(t)$ and $X(t)$. A missing sample in $m(t)$ contributes to both $C_{XM}(t, \tau)$ and $C_{MX}(t, \tau)$ terms, yielding two crossing lines in the IAF domain. Because both the TFD and the AF are related with the IAF by the one-dimensional (1-D) Fourier transform, the missing samples in the IAF domain yields undesirable artifacts in the TFD and AF domains [8].

B. Demonstration Example

For clear understanding of the effect of missing samples, we first show the joint-variable representations for an FM signal without missing samples. Then, the case of random missing samples is demonstrated. Afterwards, we show the case with gapped data, which is the main focus of this paper.

A single FM signal is considered for simple and clear illustrations. Its phase trajectory, which is unknown to the receiver, is given by

$$\phi(t) = 0.05t + 0.05t^2/T + 0.1t^3/T^2, \tag{11}$$

for $t = 1, ..., T$, where T is chosen to be 128.

Fig. 1(a)–a(d) respectively show the real-part of the waveform, the WVD, the AF, and the IAF of the FM signal. No noise is added. The IAF is only computed in the diamond region because values outside this region are unavailable due to zero-padding of the time-domain data in evaluating the IAF. For the underlying single FM signal case, the magnitude of the IAF is constant within the diamond-shaped region. It is observed that the WVD shows a clear signal TF signature, with the exception of cross-term contamination in the central portion. The AF has a peak value in the origin, and exhibits a broadened slope corresponding to the IF laws of the FM signal.

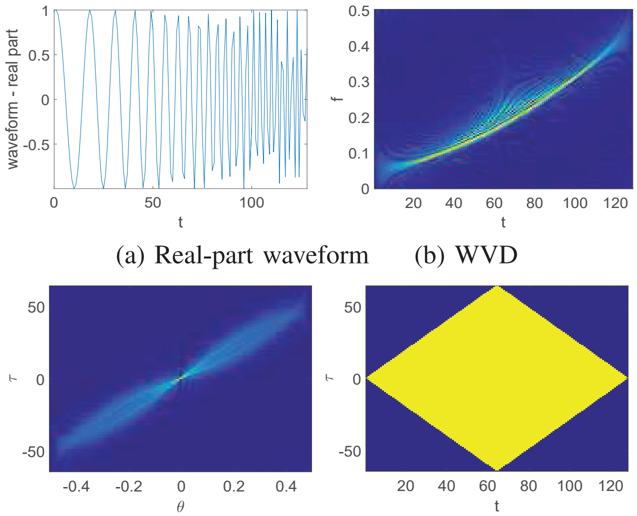

(a) Real-part waveform (b) WVD

(c) AF (d)IAF

Fig. 1 Real-part waveform, WVD, AF, and IAF of a single-component FM signal without missing samples.

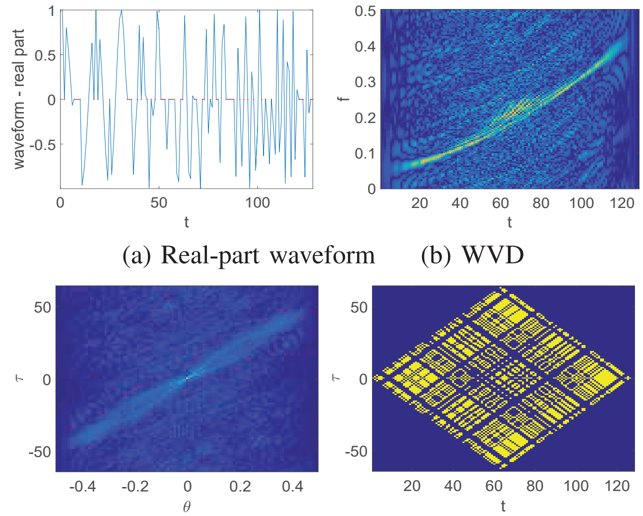

(a) Real-part waveform (b) WVD

(c) AF (d)IAF

Fig. 2 Real-part waveform, WVD, AF, and IAF of a single-component FM signal with 37.5% randomly missing samples.

In Fig. 2, we show the results when 37.5% of the samples (48 samples) are randomly missing. The missing samples are generated using the uniform distribution. In this case, it is verified that each missing sample in the time-domain waveform causes two diagonal missing lines in the IAF. The missing samples collectively yield a high level of undesired artifacts in both the WVD and AF domains with . Note that such artifacts cannot be improved by increasing the signal power.

Fig. 3 shows the results when the same number samples are missing but in a gapped manner. In this example, the missing samples occur as 8 gapped blocks, and the length of each block is 6 samples. Because of the gapped missing samples considered herein, the IAF missing samples appear as gapped as well. In this case, we observe clear aliased structures of artifacts in the WVD and AF near the original auto-terms. Because each gap contains 6 samples which act as a rectangular window, the aliasing exhibits a sinc function-like pattern. The actual energy of the alias fluctuates because of the superposition of the effect of multiple gapped missing sample groups. Comparing the results depicted in Figs. 2 and 3, there exists a clear difference between the random missing sample case and the gapped missing sample case.

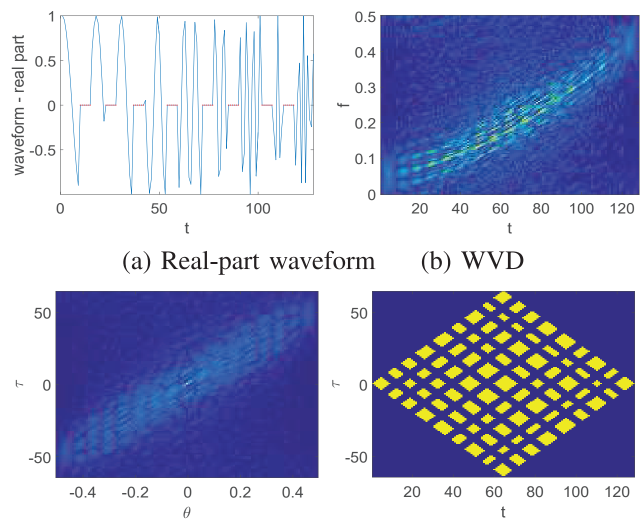

(a) Real-part waveform (b) WVD

(c) AF (d)IAF

Fig. 3 Real-part waveform, WVD, AF, and IAF of a single-component FM signal with 37.5% gapped missing samples.

C. Mitigating Effect of Missing Samples – TF Kernel Approach

In [8], robust QTFD construction of FM signals with random missing samples is considered. The method proposed therein mitigates the effect of missing samples by applying a TF kernel to the joint-variable representations. TF kernels are multiplicative filters in the ambiguity domain and translate to 2-D convolution (smoothing) in the TF domain to reduce the effect of artifacts. TF kernels can be classified into fixed (signal-independent) and adaptive (signal-dependent). A large class of signal-independent kernels, commonly known as the Cohen's class of TFDs, are available [5]. On the other hand, adaptive kernels, such as the commonly used adaptive optimal kernel (AOK) [14] and the recently developed adaptive directional TF distribution (ADTFD) [15], generally yield better results than the fixed kernels.

Fig. 4(a) shows the QTFD, after applying the AOK, for the signals with the 37.5% random missing samples, as depicted in Fig. 2. It is clear that the effect of missing samples is significantly reduced and a relatively clean TFD is achieved. Fig. 4(b) shows the QTFD of the same signal after the ADTFD is applied. The artifacts due to missing samples are also mitigated with a higher residual around the signal IFs. Figs. 4(c) and 4(d) show the corresponding results for the gapped missing case. While the effect of artifacts is again significantly reduced as compared to the WVD counterparts, respectively shown in Figs. 2(b) and 3(b), the residual effect is higher than the results obtained in the case of random missing samples, as shown in Figs. 4(a) and 4(b).

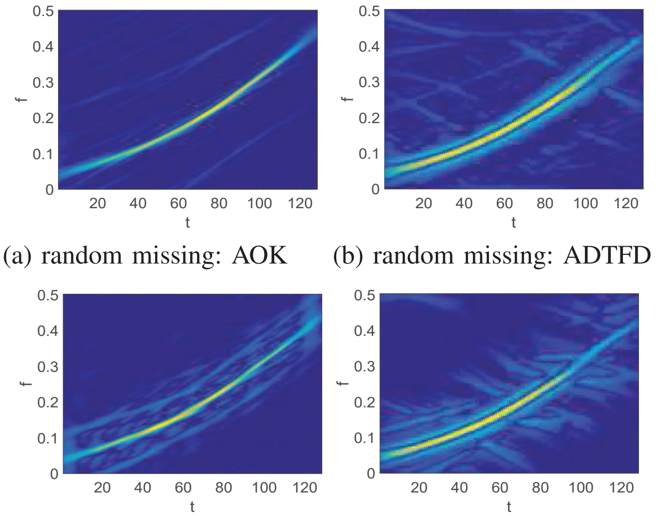

(a) random missing: AOK (b) random missing: ADTFD

(c) gapped missing: AOK (d) gapped missing: ADTFD

Fig. 4 TFD using AOK and ADTFD for FM signal with 37.5% randomly missing samples and 37.5% gapped missing samples.

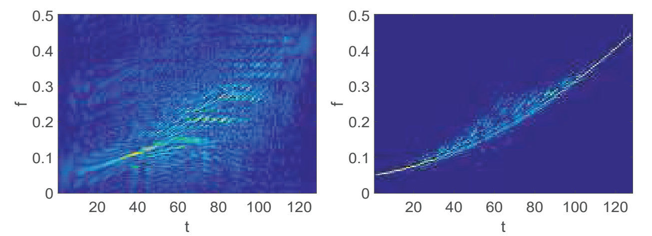

(a) applied to time-domain data (b) applied to IAF

Fig. 5 WVD of reconstructed signal using the proposed method for the FM signal with 37.5% gapped missing samples.

D. Mitigating Effect of Missing Samples – Data Interpolation

An alternative approach is to fill the missing samples through data interpolation based on a discrete set of known data. In [13], a missing data iterative adaptive approach (MIAA) is develop to fill the missing samples for *stationary* signals. The MIAA approach works well for arbitrary data missing patterns, such as gapped missing data samples as well as for uniform or non-uniform sampling, provided that the original signals are stationary. In addition, MIAA can be used for both interpolation and extrapolation of data sequences. The concept behind the MIAA approach is sequential estimation of the Capon spectrum that minimizes the weighted least squares between the received signal vector and the estimates. Then, missing samples are recovered based on the estimated frequencies and their coefficients. The Capon spectrum estimation and missing sample recovery can be iterated for performance improvement.

However, because the MIAA approach is designed for stationary signals, it does not work properly for nonstationary FM signals. Consider the single-component FM signal as depicted in Fig. 3 with 37.5% gapped missing samples. In Fig. 5(a), we show the WVD of the recovered data after the MIAA approach is applied to the time-domain FM signal waveform. The result is very poor with even higher artifact spreading than the WVD shown in Fig. 3(b).

IV. Proposed Methods

A. Obtaining TFD Using Interpolated IAF

As we discussed earlier, while the FM signals are nonstationary, the IAF is stationary with respect to the time delay. As such, we propose the application of the MIAA approach to each column (time instant) of the IAF matrix, which is stationary. Further, in lieu of the Capon estimator used in the MIAA method, we can also use sparse reconstruction methods, in the context of compressive sensing, for spectrum estimation.

Fig. 5(b) shows the improved WVD corresponding to the IAF obtained after the IAF is interpolated and extrapolated using the MIAA approach. The resulting WVD shows significant improvement as compared to Fig. 3(b), 4(c), 4(d), and 5(a). The improved WVD is generally clean except for the cross-terms, which are also observed in Fig. 1, because no kernels are applied. That is, the effect of gapped missing samples is substantially suppressed.

B. Obtaining TFD Using Sparse Reconstruction

As the signals are sparse represented in the TF domain, sparse reconstruction methods have found useful for TFD reconstruction. Denote $\mathbf{c}_{\mathbf{xx}}^{[t]}$ as a vector that contains all IAF entries along the τ dimension corresponding to time t, and $\mathbf{d}_{\mathbf{xx}}^{[t]}$ as a vector collecting all the QTFD entries for the same time t. Note that $\mathbf{c}_{\mathbf{xx}}^{[t]}$ may denote the original IAF, which corresponds to the WVD, or its smoothed version as a result of applying a kernel and missing sample recovery. Then, these two vectors are related by the IDFT with respect to f, expressed as

$$\mathbf{c}_{\mathbf{xx}}^{[t]} = \mathbf{G}_f \mathbf{d}_{\mathbf{xx}}^{[t]}, \quad \forall t, \tag{12}$$

where $\mathbf{G}_f$ is a matrix performing the IDFT with respect to f.

Because the signals are sparsely represented in the TF domain, the non-zero entries of $\mathbf{d}_{\mathbf{xx}}^{[t]}$ can be reconstructed through sparse signal recovery techniques. The problem is formulated as the following l_1-norm optimization problem,

$$\min ||\mathbf{d}_{\mathbf{xx}}^{[t]}||_1 \quad \text{s.t.} \quad \mathbf{c}_{\mathbf{xx}}^{[t]} - \mathbf{G}_f \mathbf{d}_{\mathbf{xx}}^{[t]} = 0, \quad \forall t. \tag{13}$$

In this paper, we use the orthogonal matching pursuit (OMP) [16] at each time instant. OMP is computationally attractive and allows us to specify the number of non-zero entries (i.e., iterations) in each time instant. Other methods can also be used for this purpose. For example, at the expense of a higher computationally complexity, the Bayesian compressive sensing methods [17, 18] generally yield a better TF reconstruction performance and further allow consideration of the continuous pattern of the TF signatures [19].

C. Simulation Results

Fig. 6(a) shows the sparse reconstruction results of the TFD, which is based on the same IAF as used in Fig. 5(b). The results truly follow the IFs, and a sharp TFD is achieved at all time instants due to IAF extrapolation. Some perturbation remains in the central portion due to cross-term effects. To reduce the effect of cross-terms, we can apply TF kernels after the gapped missing samples are filled and before performing OMP for TFD reconstruction. Fig. 6(b) shows such results

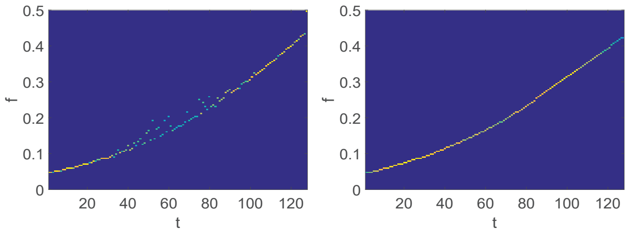

(a) no kernel applied (b) applied ADTFD before OMP

Fig. 6 Reconstructed TFD from OMP method for the FM signal with 37.5% gapped missing samples.

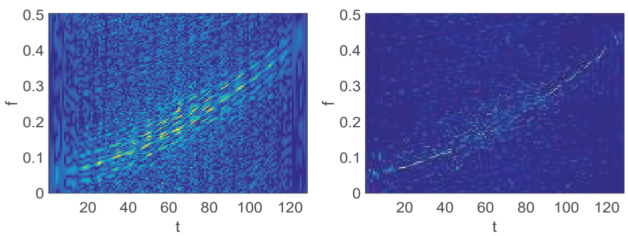

(a) WVD (b) WVD with MIAA

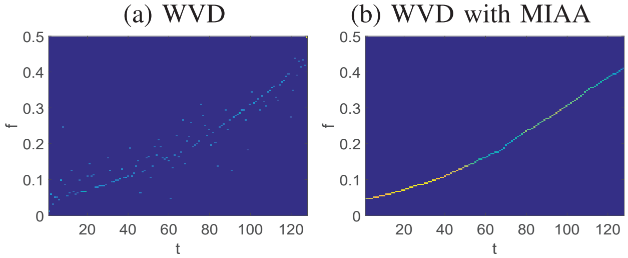

(c) OMP with MIAA (d) OMP with MIAA and ADTFD

Fig. 7 Reconstructed TFD from different methods for the noisy FM signal with 37.5% gapped missing samples (input SNR = 5 dB).

from the OMP with the application of the ADTFD, where the cross-term effect is clearly removed.

In the next example, we demonstrate the effectiveness of the proposed method in the presence of noise. The FM signal and the gapped missing sample pattern remain the same except that a noise that yields a 5 dB input signal-to-noise ratio (SNR) is added. Fig. 7 shows the WVD without missing sample recovery and kernel, WVD obtained from the IAF with missing sample recovery using MIAA, the TFD obtained using OMP from the IAF with missing sample recovery using MIAA, and the TFD obtained using OMP from the IAF with both MIAA-based missing sample recovery and ADTFD kernel filtering. It is clear that the noise cause much higher perturbation in the WVD with and without applying the MIAA for missing sample recovery, as seen in Figs. 7(a) and 7(b). The OMP result depicted in Fig. 7(c) is also degraded as compared to the noise-free case. However, further applying the ADTFD kernel enables restoration of the continuous IF signature, as shown in Fig. 7(d).

V. Conclusions

In this paper, we have developed novel algorithms to achieve resilient quadratic TF analysis for nonstationary FM signals with gapped missing samples. The proposed techniques utilize the stationarity of the IAF, and missing data recovery methods developed for stationary signals are applied to recover missing entries in the IAF. TFDs are then obtained using the Fourier relationship between the IAF and TFD, which can be either directly implemented or applied using sparse reconstruction techniques.

References

[1] A. Papandreou-Suppappola (Ed.), *Applications in Time-Frequency Signal Processing*. CRC Press, 2002.

[2] M. Skolnik (Ed.), *Radar Handbook, 3rd Ed.*. McGraw-Hill, 2008.

[3] V. Chen and H. Lin, *Time-Frequency Transforms for Radar Imaging and Signal Analysis*. Artech House, 2002.

[4] V. Chen, *The Micro-Doppler Effect in Radar*. Artech House, 2010.

[5] L. Cohen, "Time-frequency distributions – A review," *Proc. IEEE*, vol. 77, no. 7, pp. 941–981, July 1989.

[6] P. Flandrin, *Time-Frequency/Time-Scale Analysis*. Academic Press, 1999.

[7] B. Boashash (Ed.), *Time-Frequency Signal Analysis and Processing, 2nd Ed.*. Academic Press, 2016.

[8] Y. D. Zhang, M. G. Amin, and B. Himed, "Reduced interference time-frequency representations and sparse reconstruction of undersampled data," in *Proc. European Signal Process. Conf.*, Marrakech, Morocco, Sept. 2013.

[9] B. Jokanovic, M. G. Amin, Y. D. Zhang, and F. Ahmad, "Time-frequency kernel design for sparse joint-variable signal representations," in *Proc. European Signal Process. Conf.*, Lisbon, Portugal, Sept. 2014.

[10] L. Stankovic, S. Stankovic, I. Orovic, and Y. D. Zhang, "Time-frequency analysis of micro-Doppler signals based on compressive sensing," in M. G, Amin (Ed.), *Compressive Sensing for Urban Radars*. CRC Press, 2014.

[11] B. Jokanovic and M. G. Amin, "Reduced interference sparse time-frequency distributions for compressed observations," *IEEE Trans. Signal Process.*, vol. 63, no. 24, pp. 6698–6709, Dec. 2015.

[12] M. G. Amin, B. Jakonovic, Y. D. Zhang, and F. Ahmad, "A sparsity-perspective to quadratic time-frequency distributions," *Digital Signal Process.*, vol. 46, pp. 175–190, Nov. 2015.

[13] P. Stoica, J. Li, and J. Ling, "Missing data recovery via a non-parametric iterative adaptive approach," *IEEE Signal Process. Lett.*, vol. 16, no. 4, pp. 241–244, April 2009.

[14] D. L. Jones and R. G. Baraniuk, "An adaptive optimal-kernel time-frequency representation, *IEEE Trans. Signal Process.*, vol. 43, no. 10, pp. 2361-2371, Oct. 1995.

[15] N. Khan and B. Boashash, "Multi-component instantaneous frequency estimation using locally adaptive directional time frequency distributions," *Int. J. Adaptive Control and Signal Process.*, vol. 30, pp. 429-442, March 2016.

[16] J. A. Tropp and A. C. Gilbert, "Signal recovery from random measurements via orthogonal matching pursuit," *IEEE Trans. Info. Theory*, vol. 53, no. 12, pp. 4655–4666, Dec. 2007.

[17] S. Ji, Y. Xue, and L. Carin, "Bayesian compressive sensing," *IEEE Trans. Signal Proc.*, vol. 56, no. 6, pp. 2346-2356, June 2008.

[18] Q. Wu, Y. D. Zhang, M. G. Amin, and B. Himed, "Complex multitask Bayesian compressive sensing," in *Proc. IEEE ICASSP*, Florence, Italy, May 2014, pp. 3375-3379.

[19] Q. Wu, Y. D. Zhang, and M. G. Amin, "Continuous structure based Bayesian compressive sensing for sparse reconstruction of time-frequency distributions," in *Proc. Int. Conf. Digital Signal Process.*, Hong Kong, China, Aug. 2014, pp. 831–836.